SUPPORTING MATERIAL

The conformational flexibility of the carboxy terminal residues 105-114 is a key modulator of the catalytic activity and stability of Macrophage Migration Inhibitory Factor (MIF)

Farah El-Turk[1], Michele Cascella[2], Hajer Ouertatani-Sakouhi[1], Raghavendran Lakshmi Narayanan[3], Lin Leng[4], Richard Bucala[4], Markus Zweckstetter[3], Ursula Rothlisberger[2], and Hilal A. Lashuel[1]*

FIGURE S1 Rational for C-terminal deletion and insertions mutants. (A-B) Cartoon representations of three-dimensional structure of wt huMIF illustrating intersubunit interactions involving the C-terminal region 105-114. The intermolecular antiparallel β-sheet between β-strand β3 of one monomer and the edge β-strand β2 of the neighbouring monomer are highlighted in red (A). This β-sheet is stabilized mainly by hydrogen bond interactions between residues Val39 (in β2, monomer 1) and Ala48 (in β3, monomer 2). (B) The C-terminal β-hairpin comprising residues 105-114 is involved in several intersubunit interactions and could contribute to trimer stabilization through two types of contacts: i) intersubunit β-sheet formation mediated by hydrogen bonding between Asp105 and Gly107 in the C-terminal β-strand β6 and Ile96 and Tyr98 within the inner β-strand β5 of the neighbouring subunit, ii) by a salt-bridge interactions between the carboxylate group of the C-terminal residue Ala114 and the side-chain of Arg73, located on the α-helix H2 of the neighbouring subunit. (C) Schematic representation of the interactions between the different subunits within the trimer wt huMIF. To determine the contribution of the hydrogen bonding interactions between Ala48 (β3) and Val39 (β2) (A), we generated a mutant in which Ala48 was replaced by the secondary structure breaker proline residue (A48P). To probe the importance of the salt bridge interaction between Ala114 and Arg73, we generated a mutant where the last five amino acids (ΔNSTFA, ΔC5 huMIF$_{1\text{-}109}$), corresponding to the β–strand β7 were removed. We hypothesized that this would significantly increase the distance between the two interacting groups and disrupt the formation of the salt-bridge. To determine the effect of disrupting all stabilizing interactions involving the C-terminal β-strands (salt bridge interaction between Ala114 and Arg73 as well as the intersubunit hydrogen bonds between β–strands β6 and β5), we generated a mutant where the entire β–hairpin comprising the β–strands β6 and β7 (ΔNVGWNNSTFA, ΔC10 huMIF$_{1\text{-}104}$) was removed. Figures were generated with VMD (Visualization Molecular Dynamics) software, using the pdb 1GD0 (resolution 1.5Å) corresponding to human MIF (*24*).

FIGURE S2 Structural distortion of α-helix H2 upon elision of the C-terminus: structure of one single monomer of ΔC5 huMIF$_{1\text{-}109}$ during MD simulations. The α-helices are coloured in magenta, 3-10

helices in blue. The black circle highlights the structural modifications occurring in H2. Similar distortion is observed during the MD simulations of ΔC10 huMIF$_{1-104}$ mutant.

FIGURE S3 Thermal stability studies using far UV circular dichroïsm at multiple protein concentrations. Far UV/CD spectra (A-C) and thermal denaturation (D-F) of wt huMIF, ΔC5 huMIF$_{1-109}$ and ΔC10 huMIF$_{1-104}$ respectively, in PBS 1X, pH 7.4, at 2.5 μM (black line), 5 μM (blue line), 15 μM (green line) and 50 μM (red line).

FIGURE S4 Analytical ultracentrifugation sedimentation velocity analyses at multiple protein concentrations. (A-C) Sedimentation coefficients distributions of wt huMIF (A), ΔC5 huMIF$_{1-109}$ (B) and ΔC10 huMIF$_{1-104}$ (C) were obtained from analysis of the sedimentation profiles at 5 μM (blue line), 15 μM (red line) and 50 μM (green line), using the c(s) distribution as a variant of Lamm equation solutions using SEDFIT as described in materials and methods. (D) c(M) distribution of wt huMIF (solid line), ΔC5 huMIF$_{1-109}$ (dashed line) and ΔC10 huMIF$_{1-104}$ (dotted line) at 15 μM.

FIGURE S5 Characteristic contacts of HPP in the MIF catalytic pocket. The substrate is drawn in ball-and-stick; the catalytic residues are drawn in licorice. Structural data according to (*24*).

FIGURE S1

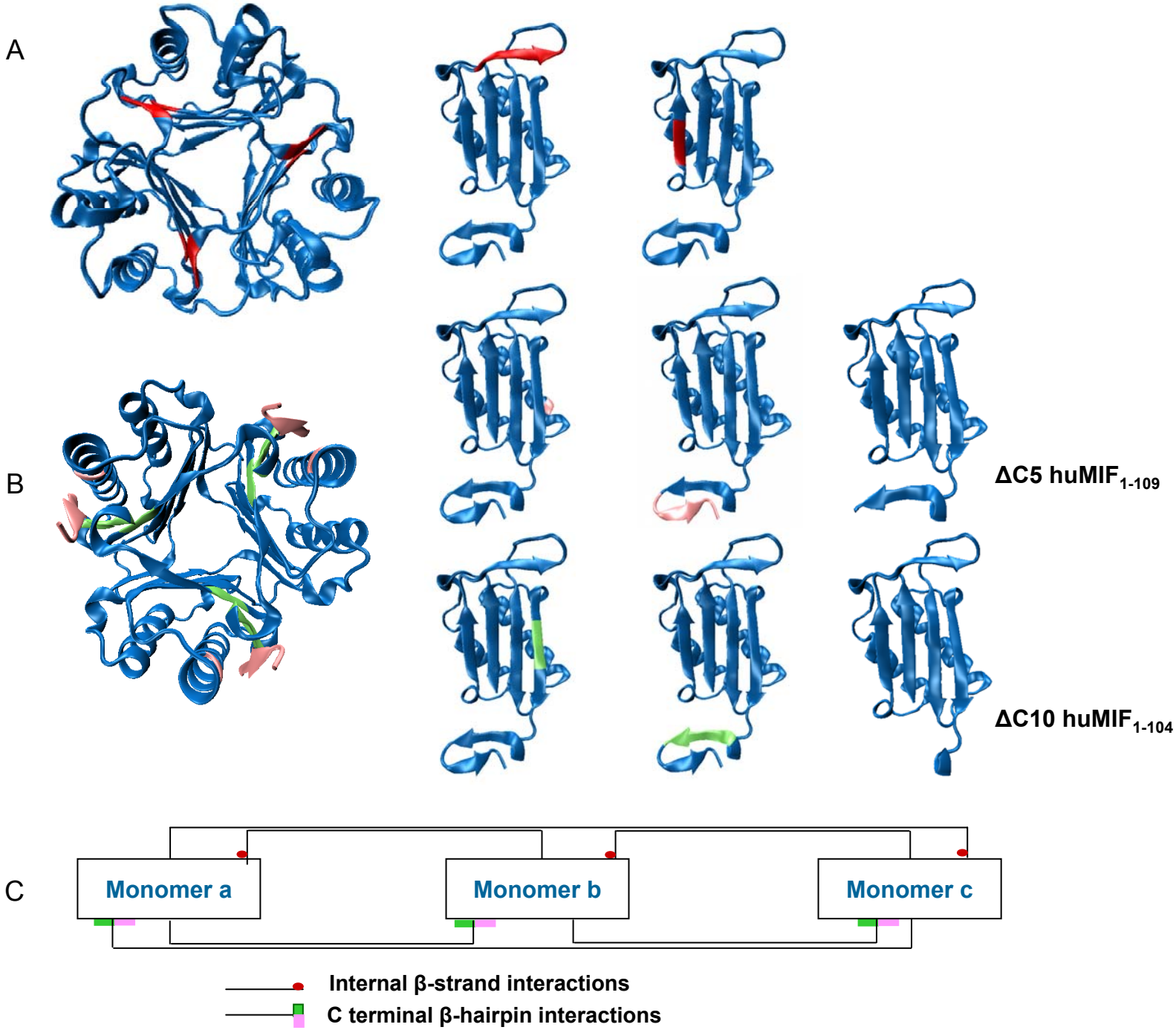

El-Turk & Lashuel, *et al.* (2008)

FIGURE S2

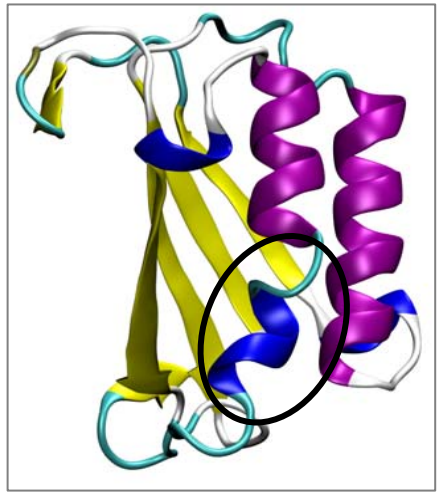

El-Turk & Lashuel, *et al.* (2008)

FIGURE S3

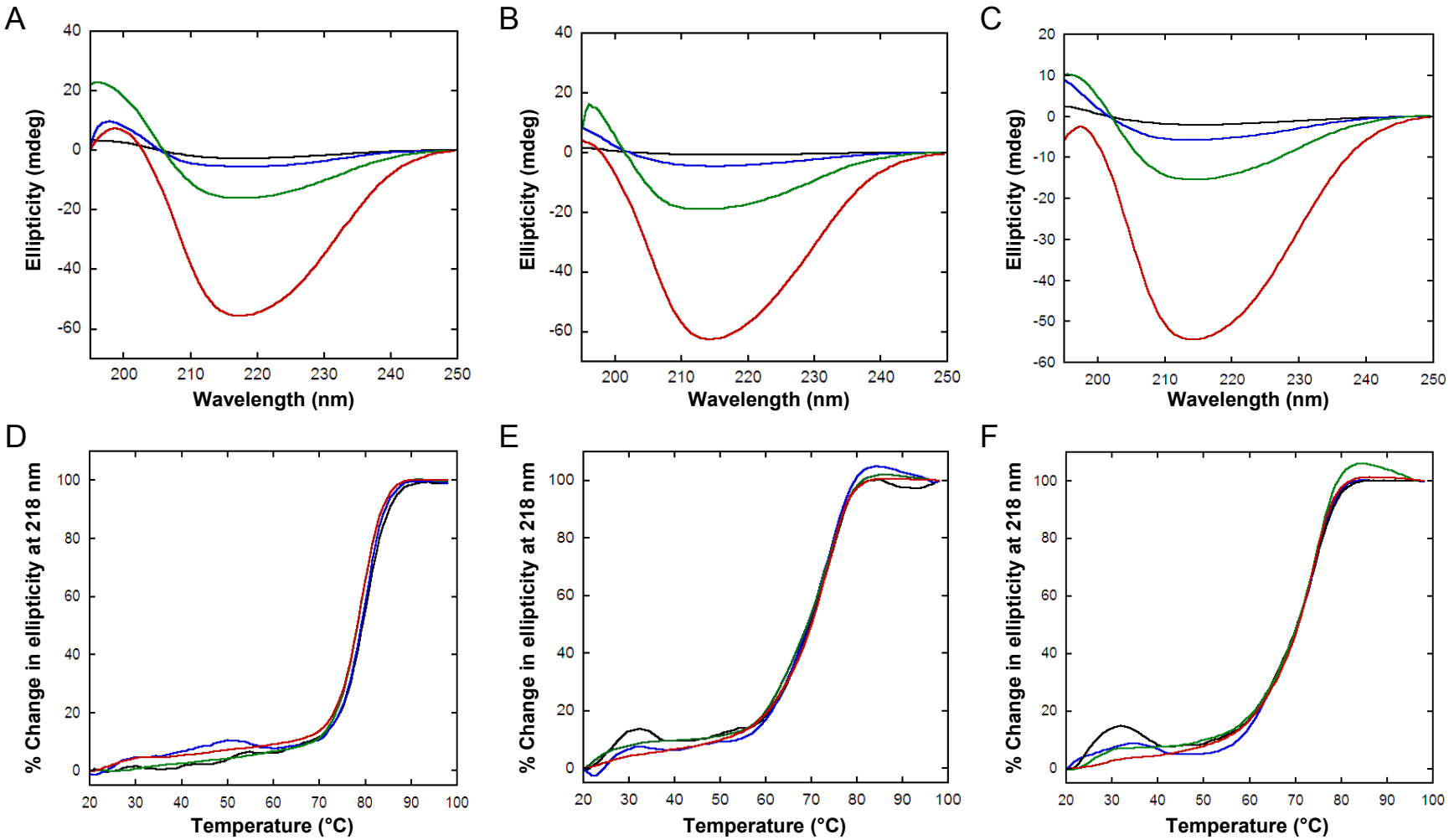

El-Turk & Lashuel, *et al.* (2008)

FIGURE S4

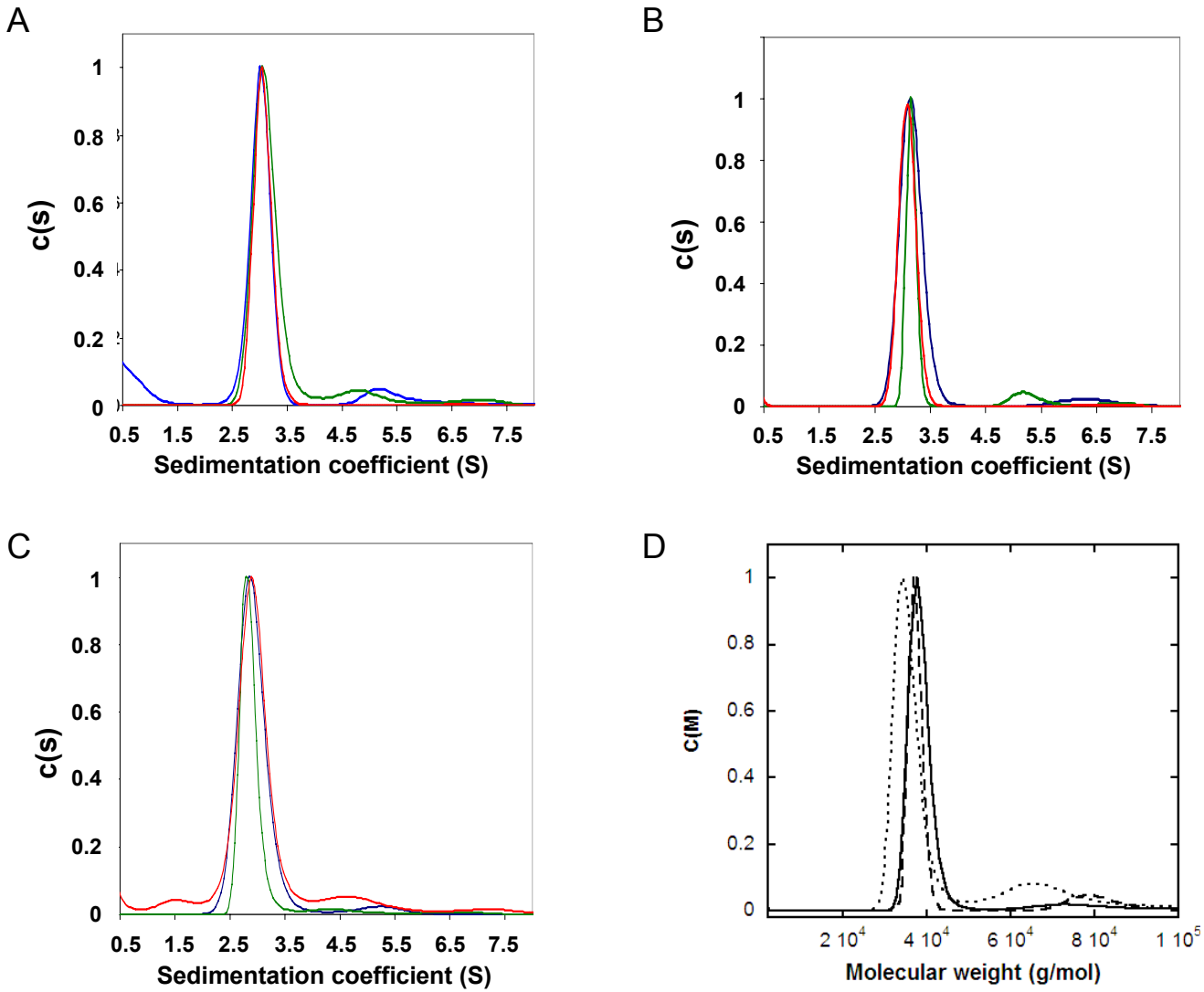

El-Turk & Lashuel, *et al.* (2008)

FIGURE S5

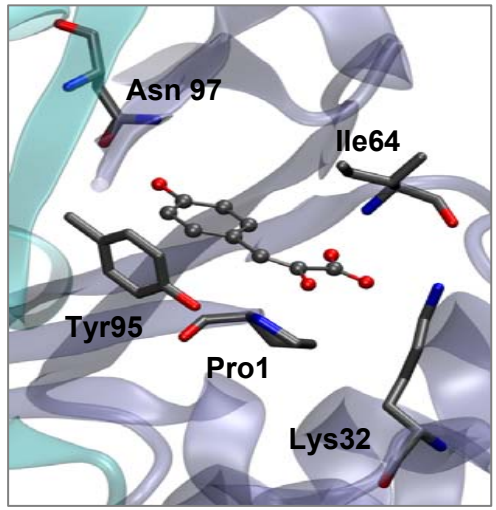

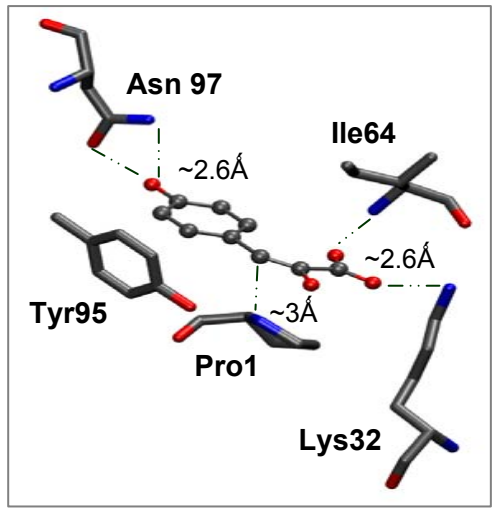

El-Turk & Lashuel, *et al.* (2008)